Polymer Chemistry

ROYAL SOCIETY OF CHEMISTRY

PAPER

View Article Online
View Journal | View Issue

Cite this: *Polym. Chem.*, 2023, **14**, 1743

Bioactive polyethylene synthesized by ring opening metathesis polymerization for potential orthopaedic applications†

Jiayi Guo, [a] Eun Ju Park,[a] Yew Chin Teo, [a] Asyraf Abbas,[a] Denise Goh, [b] Raymond Alexander Alfred Smith, [c] Yuntong Nie,[d] Hang T. L. Nguyen,[d] Joe Poh Sheng Yeong,[b] Simon Cool,[b,c] Haruyuki Makio[e] and Peili Teo *[a]

Received 9th December 2022,
Accepted 20th March 2023

DOI: 10.1039/d2py01545e

rsc.li/polymers

Efficient synthesis and bioevaluation of novel brush-type polyethylene-peptide copolymers for potential applications in orthopaedic implants are described here. The brush-type copolymers containing pendant arms of polyethylene (PE) and PEGylated biomolecules including linear arginyl-glycyl-aspartic acid (RGD) and collagen fragments $(Gly\text{-}Pro\text{-}Hyp)_3$ were synthesized by ring-opening metathesis polymerization (ROMP) using the well-defined 2nd generation Grubbs' ruthenium catalyst. The random copolymerization of two separate norbornene-dicarboxylic anhydride macromonomers allowed for the incorporation of hydrophilic PEGylated biomolecules into hydrophobic polyethylene. Thermal stability of this polyethylene-peptide copolymer was also markedly improved for melt extrusion-based material processing. The copolymers were blended with ultra-high molecular weight polyethylene (UHMWPE), extruded into filaments and 3D-printed into sheets using fused filament fabrication methods. The ability of these polyethylene materials to enhance osteogenic activity whilst reducing inflammatory response compared to pure UHMWPE was evaluated by the *in vitro* alkaline phosphatase (ALP) assay and an *in vivo* murine model study, respectively. The results presented here serves as a promising guide for biofunctionalization of polyethylene materials for potential orthopaedic applications.

1 Introduction

Synthetic polymers such as polyethylene (PE), polycaprolactone (PCL) and poly(methyl methacrylate) (PMMA) are important materials used in the biomedical fields.[1,2] Amongst these, polyethylene (PE) is the most common polymer used in medical implant fabrication due to its desired mechanical properties, inertness, and nontoxicity.[3] Yet, foreign body responses on PE-based medical devices have been widely reported,[4] resulting in extensive research into improving the biocompatibility of polyethylene.[5] Some of the current methods used to improve the biocompatibility of PE include blending of biomolecules into the base polymer.[6,7] However, this method has disadvantages of potential phase separation or premature thermal degradation of biomolecules during material processing that requires heat.[8,9]

The arginyl-glycyl-aspartic acid (RGD) sequence is the minimal binding domain for fibronectin to recognize cell surface integrins.[10] Materials modified with RGD peptides have been reported to facilitate cell adhesion, migration and proliferation.[11] Apart from RGD, collagen is found in the extracellular matrix, particularly in skin, cartilage and bone. The use of collagen in implants targeting tissue regeneration has been studied over the years. Collagen fragments bearing glycine, proline and hydroxyproline sequences $(GPHyp)_3$ have also been shown to promote skin cell adhesion, migration, differentiation and proliferation.[12–14] Despite the apparent usefulness of these biomolecules for improving biocompatibility and potentially inducing tissue regeneration in implants,[15] these short peptide sequences tend to have low thermal stability, are hygroscopic and lack mechanical strength, making their use in medical devices challenging. Therefore, in order to

[a]*Institute of Materials Research and Engineering (IMRE), Agency for Science, Technology and Research (A*STAR), 2 Fusionopolis Way, Innovis #08-03, Singapore 138634, Republic of Singapore . E-mail: teo_peili@imre.a-star.edu.sg*
[b]*Institute of Molecular and Cell Biology (IMCB), Agency for Science, Technology and Research (A*STAR), 61 Biopolis Drive, Proteos, Singapore 138673, Republic of Singapore*
[c]*School of Chemical Engineering, The University of Queensland, Brisbane, QLD 4072, Australia*
[d]*Mitsui Chemicals Singapore R&D Centre, Pte. Ltd, 50 Science Park Road, #06-08 The Kendall, Singapore 117406*
[e]*R&D Center, Mitsui Chemicals, Inc., 580-32 Nagaura, Sodegaura, Chiba 299-0265, Japan*

† Electronic supplementary information (ESI) available. See DOI: https://doi.org/10.1039/d2py01545e

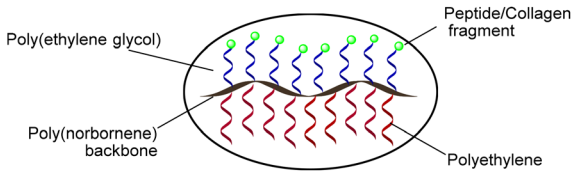

Fig. 1 Schematic of a bioactive polyethylene-peptide brush copolymer.

improve the usability of these short peptides in medical device fabrication, methods to improve their stability would be necessary.

Ring-opening metathesis polymerization (ROMP) of norbornene (NB) derivatives is a versatile method for functional polymer synthesis. Grubbs and co-workers have demonstrated that a polynorbornene backbone is non-toxic[16–18] and RGD-functionalized polynorbornenes constructed by ROMP can facilitate cell proliferation.[11] Recently, we have reported on bioactive PCL-peptide and PLA-peptide brush copolymers for bone-tissue engineering.[19] Inspired by these positive outcomes, we sought to utilize ROMP to construct peptide-containing bioactive polyethylene copolymers for use as bioadditives in orthopaedic materials. Herein, we report the preparation of a series of "bioactive polyethylene" brush copolymers *via* ROMP, consisting of PE side chains and PEGylated RGD or $(GPHyp)_3$ (Fig. 1). The "bioactive polyethylene" was formulated with ultra-high molecular weight polyethylene (UHMWPE) and 3D-printed into coupons for biovalidation *in vitro* and *in vivo*. It functions as a carrier for thermally sensitive biomolecules in high-melting point polymers such as UHMWPE. Also, the biocompatibility of UHMWPE is improved using this "bioactive polyethylene" without premature degradation of the biomolecules RGD or $(GPHyp)_3$, which are present in the final PE formulation.

2 Experimental section

2.1 Polymer synthesis and characterization

Macromonomers (MMs) **I** and **II**, where **I** is a PEGylated RGD or $(GPHyp)_3$ macromonomer, and **II** is a PE-based macromonomer, were created independently. **I** and **II** are then copolymerized together in a random fashion, using a 2nd generation Grubbs' catalyst [**G2**], in a nitrogen-filled glovebox.[20,21] Brief descriptions of the polymer syntheses are presented below. The conversion of **I** and incorporation of **II** in the final brush copolymers were determined by analyzing ^{1}H NMR spectra according to the characteristic signals of the norbornene-terminated PE and PEG side chains, respectively. The PDIs and average molecular weights (M_n) of PE copolymers were calculated by high-temperature gel permeation chromatography (HT-GPC). For detailed chemical synthesis and characterization data, please refer to the ESI.†

2.1.1 Synthesis of peptide-based macromonomer I. Polyethylene glycol (PEG) diamine of various chain lengths (MW 1000 and 3400) can be reacted with *cis*-norbornene-*exo*-2,3-dicarboxylic anhydride in refluxing toluene to create the main macromonomer body, NBPEG (**1**).[22,23] Once NBPEG (**1**) is created, we add on the peptides by means of condensation reactions in the presence of hydroxybenzotriazole (HOBt), 3-[bis(dimethylamino)methyliumyl]-3*H* benzotriazol-1-oxide hexafluorophosphate (HBTU) and *N*,*N*-diisopropylethylamine (^{i}Pr$_2$EtN) to form an amide linkage between the amine terminal on NBPEG and the carboxylic acid terminal of the peptide. The molecular weights of the obtained peptide-based macromonomers (**Ia–d**) can be varied from 1500 to over 4000 by adjusting the PEG chain and the corresponding peptides (Scheme 1). **Ia–d** will serve as the bioactivity-conferring macromonomers in the subsequent brush copolymer formation by ROMP (Scheme 3).

2.1.2 Synthesis of polyethylene-based macromonomer II. To obtain a primary amine terminus on polyethylene (PE) for macromonomer formation, a condensation reaction in refluxing toluene in the presence of hexamethylenediamine (HMDA) was carried out on succinic acid-terminated polyethylene (SA-t PE) (MW 1400 and 5000), which was prepared following literature procedures.[24] Upon obtaining the amine-terminated PE (**2**), a second condensation reaction with *cis*-norbornene-*exo*-2,3-dicarboxylic anhydride afforded the PE-based macromonomers (NB-SA-t PE) (**IIa** and **IIb**) (Scheme 2) with a conversion of over 90% on SA-t PE_{1400}.[22] **IIa** and **IIb** will function as synthetic macromonomers in the brush copolymer formation *via* ROMP, as highlighted in Scheme 3.

2.1.3 General ROMP procedure using I and II to prepare PE-peptide brush copolymers III. With the macromonomers of PEGylated RGD or $(GPHyp)_3$ (**Ia–d**) and norbornene-terminated polyethylene (**IIa** and **IIb**) ready, the final PE-peptide brush copolymers (**IIIa–d**) are prepared by ROMP using 1.25 mol% of 2nd generation Grubbs' catalysts in 1,2-dichlorobenzene (1,2-DCB) at 75 °C with a molar ratio [**I** : **II**] of 1 : 5 (Scheme 3).[25]

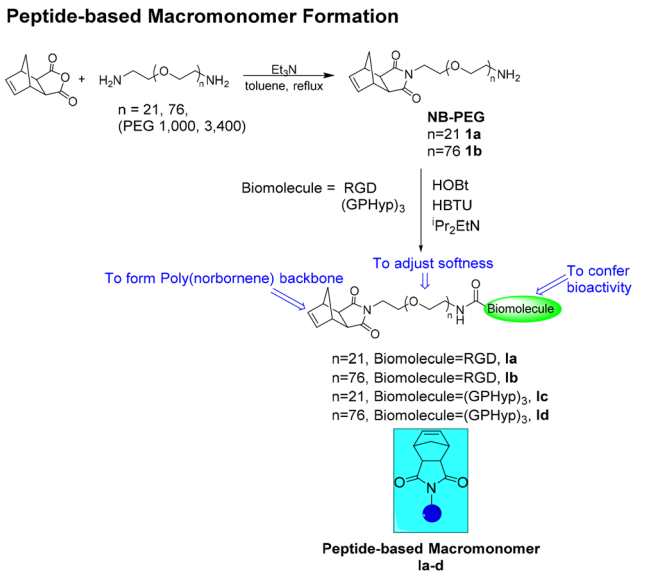

Scheme 1 Synthesis of peptide-based macromonomers **Ia–d**.

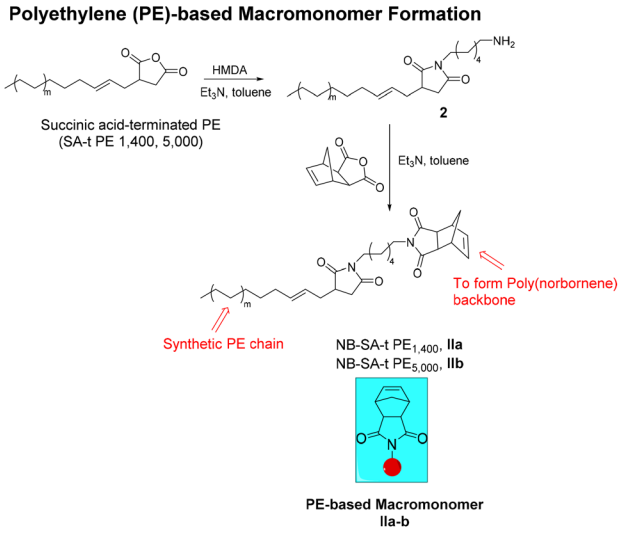

Scheme 2 Synthesis of polyethylene-based macromonomers **IIa** and **IIb**.

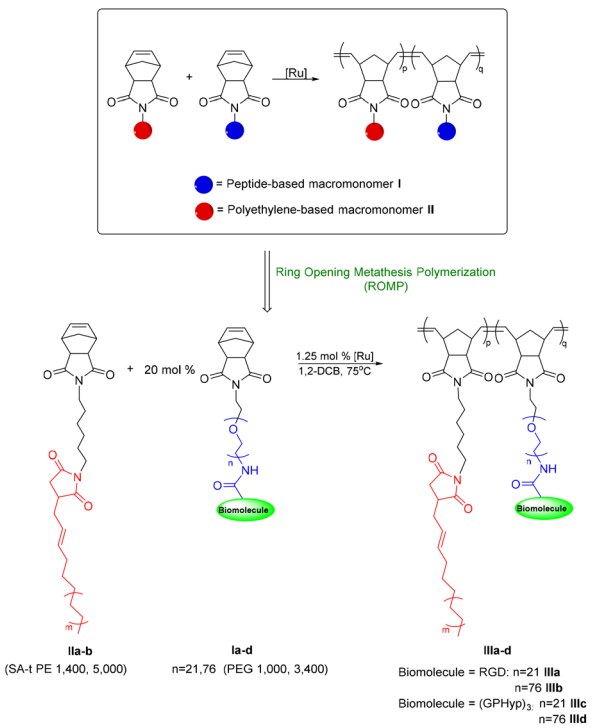

Scheme 3 General ROMP procedure for the preparation of PE-peptide brush copolymers (**IIIa–d**) where [Ru] refers to the 2nd generation Grubbs' catalysts [**G2**].

The reactions were terminated upon addition of ethyl vinyl ether. The copolymer was precipitated from methanol and repeatedly washed with acetone/H_2O. PE-mPEG with no biomolecules, which is the brush copolymer with side chains of PE and methoxy-PEG, was prepared by the same ROMP strategy. It serves as a control for PE-peptide copolymers in the biological evaluation. The formation of the desired brush copolymer was characterized by ^{1}H NMR spectroscopy, where the characteristic signals from the poly(ethylene glycol) (PEG) chain and polyethylene chains were observed, respectively.

2.2 Preparation of 3D-printed coupons

The obtained PE-peptide brush copolymers **III** were formulated as "bioadditive" (Fig. 2a) for UHMWPE supplied by Mitsui Chemicals Inc. as the base polymer to create the formulations [PE-peptide/UHMWPE]. Coupons **CIII$_{1400}$** and **CIII$_{5000}$** (Fig. 2c) were created for biological evaluation using these formulations in fused filament fabrication type 3D printing. A blending ratio of 10 wt% of **III** in UHMWPE was used, whilst filament extrusion was carried out using a Thermo Scientific 11 co-rotating twin-screw extruder to achieve an average filament diameter of 2.85 mm (Fig. 2b). Two types of PE coupons were 3D-printed using an Ultimaker S5 with printing parameters similar to those reported by Dontsov[26] and Rocha[27] but at a lower print speed to cater for *in vitro* and *in vivo* studies. The coupons for *in vitro* assays were formed with a dimension of 10 × 10 × 0.2 mm^3, while the coupons for *in vivo* assays were formed with a dimension of 5 × 5 × 0.2 mm^3.

2.3 *In vitro* alkaline phosphatase (ALP) assay

Alkaline phosphatase (ALP) is a widely recognized biochemical marker for osteoblast activity. The osteo-inductivity of exogenously applied BMP-2 (bone morphogenetic protein-2) can be measured *in vitro* using a murine myoblast cell line (C2C12). 3D-printed PE coupons **CIII** were placed in 100% ethanol for 5 minutes. Excess ethanol was removed, and the coupons were allowed to air-dry for 1 hour under a TC hood. The coupons were incubated with 100 ng BMP-2 in 200 μL of PBS for 20 minutes at room temperature with gentle agitation. The BMP-2 solution was removed, and the coupons were washed twice with 500 μL of PBS. Cells (C2C12) were harvested and seeded on the coupons at a density of 20 000 cells per cm^2 in DMEM with 5% FCS. The total protein was isolated from cells at day 4 using an ice-cold RIPA buffer. The cells were incubated for 20 minutes with the RIPA buffer, and then the cells and coupons were homogenized using a cell scraper. The insoluble material was removed *via* centrifugation (12 000*g*, 4 °C, 10 minutes), and the total protein content of the supernatant was quantified by the BCA assay. A total of 7.5 μg of protein from each sample was analysed in triplicate after the addition of pNPP solution (Thermo Fischer) and incubation at 37 °C for 1 hour or longer. Absorbance at 405 nm was measured using a

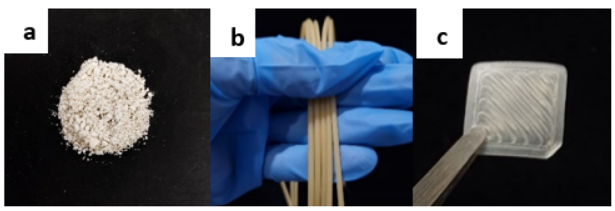

Fig. 2 (a) Bioactive polyethylene; (b) PE$_{5000}$-RGD/UHMWPE filaments (**FIII$_{5000}$**); (c) a 3D-printed PE$_{5000}$-RGD/UHMWPE coupon (**CIII$_{5000}$**).

Hidex Sense spectrophotometer. Absorbance values were normalized to no-treatment control and represent mean ± S.D. from duplicate conditions in a single experiment. The procedure was performed as previously reported.[28]

2.4 *In vivo* biocompatibility study

The *in vivo* biocompatibility study of the 3D-printed PE coupons **CIII$_{5000}$** was performed using murine models. Eight-week-old female C57BL/6 wild-type mice were purchased from InVivos Pte Ltd and randomly assigned to one of the following four groups: (1) sham, (2) PE-blank, (3) PE-RGD and (4) PE-GPHP. All groups had at least 4 mice. Briefly, each mouse was anaesthetized with ketamine/xylazine, and a small incision was made on the upper dorsal back. Coupons **CIII$_{5000}$** were then inserted into the subcutaneous space under the skin. Four weeks post-implantation, all mice were sacrificed. Mouse skin surrounding the implant was harvested, fixed in formalin and embedded in paraffin for histological studies. Hematoxylin and eosin (H&E) staining and immunohistochemistry staining for CD3 (clone SP162) were performed on these skin sections. Appropriate controls were included, and images were captured using a Zeiss Axio Scan.Z1 slide scanner. All animal handling procedures were approved by the Institutional Animal Care and Use Committee and conformed to the National Advisory Committee for Laboratory Animal Research Guidelines (IACUC #201550).

3 Results and discussion

3.1 Polymer synthesis and characterization

The random brush copolymers, where two separate macromonomers were copolymerized *via* ROMP were designed to chemically incorporate hydrophilic biomolecules into hydrophobic PE. Notably, PEG was introduced here as a linker and to adjust softness and hydrophilicity of the final copolymers. The PEG chain also ensures that the bioactive peptide motif remains sterically accessible in the final brush structure and is not buried in the matrix of the synthetic PE side chains. We term such PE copolymers as "bioactive polyethylene" (Fig. 1). This bioactive polyethylene will find much use in biomedical applications where it possesses both the bioactivity of the appended biomolecules and the thermomechanical properties of the synthetic PE side chains. In fact, incorporation of hydrophilic macromonomers into brush polymers with PE side chains is technically difficult due to the challenge of balancing the poor solubility of PE with macromonomers of widely differing properties and the high demands of techniques for its characterization. Brush-type PE copolymers are rare in the literature. Although Hadjichristidis and co-workers[29] reported one example of PE-based homobrushes, the brush polymer was homopolymerized with only norbornyl PE-based macromonomers with no biomolecules incorporated.

Due to the differing properties of peptide-based macromonomers **I** and PE macromonomers **II**, optimization of the ROMP reaction conditions for copolymerization of **I** and **II** was challenging, on its own. We began screening the copolymerization using NB-SA-t PE$_{1400}$ (**IIa**) and NB-PEG$_{1000}$-RGD (**Ia**) as representative macromonomers (Table 1). Due to the limited solubility of **IIa** in common organic solvents such as dichloromethane, THF and methanol, copolymerization had to be carried out in solvents compatible with **IIa** such as benzene and toluene at elevated temperature. Benzene at 75 °C worked as the best solvent for this ROMP, providing 13% incorporation of NB-PEG$_{1000}$-RGD (**Ia**) into copolymer **IIIa** with quantitative conversion relative to **IIa** (entry 1). A ROMP using highly active 3rd generation bis(pyridine) Grubbs' catalyst [**G3**] at 1.25 mol% with other factors unchanged was attempted but resulted in low conversion of **I** and incorporation of **Ia**. This is likely due to the low thermal stability of [**G3**]. Higher [**G2**] concentrations did not yield significant improvements in conversion or **Ia** incorporation (entries 2 and 3). Interestingly, **Ia** incorporation halved upon prolonged stirring from 24 h to 40 h (entry 4). This may be due to secondary metathesis reactions occurring during the prolonged reaction in the presence of [**G2**]. MMs with a lower molar ratio of [**I** : **II**] of [1 : 10] was attempted for reaction sustainability (entry 5). However, a decrease in **Ia** incorporation was observed. Hence, the MMs molar ratio was maintained at [1 : 5]. In view of the differing reactivities of these two MMs, we also tested the addition of **Ia** at two time points (t = 0 and 2 h) (entry 6). Only 6% incorporation of **Ia** was obtained. Thus, it is noteworthy that the reactivity of **Ia** in non-polar solvents is challenging, even with the gradual addition of the bio-macromonomer. We also explored the possibility of carrying out this reaction under atmospheric conditions. However, the incorporation of **Ia** is lowered to 4% (entry 7). Homopolymerization of these two types of macromonomers **Ia** and **IIa** under the same conditions was also carried out separately, to examine their reactivity (entries 8 and 9). Adaptability of **Ia** and **IIa** in this ROMP system varied. The PE macromonomer **IIa** showed comparatively efficient conversion (92%) compared to PEGylated macromonomer **Ia**

Table 1 ROMP condition optimization[a]

Entry	Catalyst (mol%)	[**Ia**]$_0$: [**IIa**]$_0$	Conversion[b] (%)	**Ia** Incorporation[c] (mol%)
1	1.25	[1 : 5]	>99	13
2	1.75	[1 : 5]	89	6
3	2.00	[1 : 5]	88	6
4[d]	1.25	[1 : 5]	73	3
5	1.25	[1 : 10]	88	5
6	1.25	[1 : 5][e]	83	6
7[f]	1.25	[1 : 5]	86	4
8	1.25	[100 : 0][g]	66	—
9	1.25	[0 : 100][h]	92	—

[a] Reaction was conducted in 75 °C benzene in the presence of [**G2**] under an N_2 atmosphere with [**IIa**]$_0$ = 0.05 M for 24 h. [b] Conversion was calculated by ^{1}H NMR analysis according to norbornyl protons. [c] Incorporation of **Ia** was determined by ^{1}H NMR analysis according to the PEG signal of **Ia**. [d] Reaction was conducted for 40 h. [e] 10 mol% × 2, added respectively at t = 0 and 2 h. [f] Reaction was conducted under an air atmosphere. [g] Homopolymerization of NB-PEG$_{1000}$-RGD. [h] Homopolymerization of NB-SA-t PE$_{1400}$.

(66%). This is likely due to better solubility of hydrophobic **IIa** in benzene compared to that of hydrophilic **Ia**. Hence, it is within expectations that ROMP of these two MMs together would be even more challenging.

Overall, by balancing the challenges of poor solubility of polyethylene and differing properties between **Ia** and **IIa**, we were able to achieve the optimized ROMP conditions using 1.25 mol% 2nd generation Grubbs' catalyst [**G2**] in 75 °C benzene with a molar ratio of [**I** : **II**] at [1 : 5], to achieve the optimum conversion of **IIa** and incorporation of **Ia** into the copolymer. However, in consideration of the carcinogenicity of benzene, we sought to employ a more benign solvent such as 1,2-dichlorobenzene (1,2-DCB). Fortunately, we were able to replicate the reaction outcomes under the same reaction conditions.

Upon optimizing the ROMP conditions of NB-SA-t PE_{1400} (**IIa**) and NB-PEG_{1000}-RGD (**Ia**), we extended the reaction conditions to longer chain NB-SA-t PE_{5000} macromonomer (**IIb**), longer PEG chain (MW 3400) and other PEGylated peptide macromonomers (**Ib–d**) such as collagen fragment $(GPHyp)_3$ (Table 2, entries 2–4). Good conversion of **II** (>70%) and incorporation of **I** (>3%) were obtained. Overall, bioactive PE-peptide brush copolymers **III** could be afforded by ROMP with a conversion of over 90% on NB-SA-t PE_{1400} and 70% on NB-SA-t PE_{5000}, with NB-PEG-peptide incorporation of up to 13%, using the presented strategies.

Alongside the above, PE (MW 1400 and 5000)–methoxy-PEG (MW 1000 and 5000) copolymers without biomolecules (**IV**) were also prepared under the same conditions (Table 2, entries 5 and 6). Copolymers **IV** serve as controls in the subsequent biovalidation. The higher conversion and incorporation of **I** into **IV** is due to the higher solubility of NB-methoxy-PEG in 1,2-dichlorobenzene (DCB). The syntheses of brush copolymers **III** and **IV** were subsequently scaled up to 2 g with high consistency in both conversion and biomacromonomer incorporation for further material processing.

We have also explored an alternative synthetic route to obtain **IIIa** as shown in Scheme 4. First, condensation of *cis*-norbornene-*exo*-2,3-dicarboxylic anhydride with hexamethylenediamine (HMDA) was performed to obtain a monomer (NB-HMDA) for ROMP with **Ia**, followed by grafting of SA-t PE onto the brush polymer in the final step. However, the ROMP step only gave a low yield of less than 25%. We noticed a significant amount of unreacted **Ia** and NB-HMDA after the ROMP reaction. Although the subsequent PE chain "grafting-on" can still be carried out with SA-t PE (MW 1400), it is noted that this route to obtain **IIIa** is impractical.

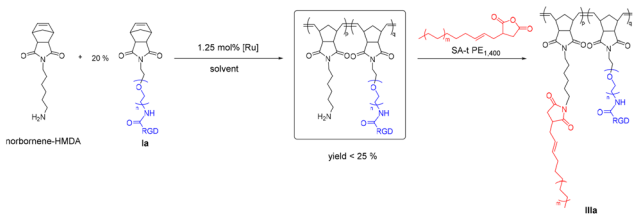

Scheme 4 Alternative synthetic route to form PE_{1400}-RGD copolymer **IIIa**, where [Ru] refers to the Grubbs' catalysts.

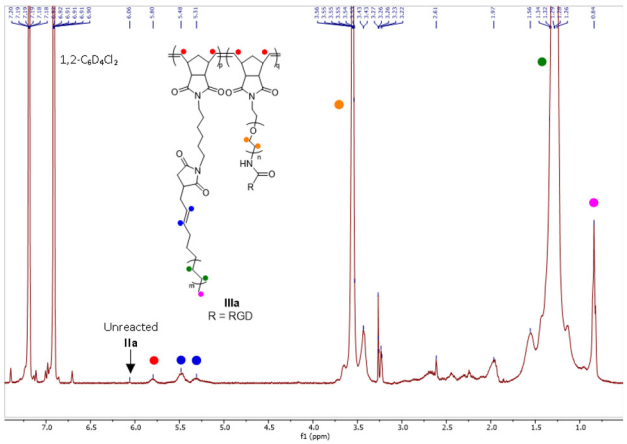

Fig. 3 ^{1}H NMR spectrum of the PE_{1400}-RGD copolymer **IIIa**.

The formation of the PE-peptide copolymer was evident from ^{1}H NMR spectroscopy. The NMR characterization of PE polymers is challenging due to its limited solubility in common deuterated organic solvents at room temperature. Finally, we managed to determine the copolymer structure from spectra recorded using d_4-dichlorobenzene ($1,2\text{-}C_4D_6Cl_2$) at 120 °C on a Bruker ASCEND cryo-400 NMR spectrometer. Using ^{1}H NMR spectra of the PE_{1400}-RGD copolymer **IIIa** (Fig. 3) as a reference, chemical shifts of vinyl protons (5.48 and 5.31 ppm), PE chains (1.29 ppm), PEG chains (3.55 ppm),

Table 2 ROMP[a] conversion and incorporation of PE-peptide brush copolymers **III**

Entry	PE MMs **II**	PEG MMs **I**	Brush copolymer **III**	Conversion[b] (%)	**I** incorporation[c] (mol%)
1	NB-SA-t PE_{1400}	NB-PEG_{1000}-RGD	**IIIa**	>99	13
2	NB-SA-t PE_{5000}	NB-PEG_{3400}-RGD	**IIIb**	72	3
3	NB-SA-t PE_{1400}	NB-PEG_{1000}-$(GPHyp)_3$	**IIIc**	>99	6
4	NB-SA-t PE_{5000}	NB-PEG_{3400}-$(GPHyp)_3$	**IIId**	77	4
5	NB-SA-t PE_{1400}	NB-methoxy-PEG_{1000}	**IVa**	>99	12
6	NB-SA-t PE_{5000}	NB-methoxy-PEG_{5000}	**IVb**	99	4

[a] Reaction was conducted in 75 °C 1,2-dichlorobenzene (1,2-DCB) in the presence of 1.25 mol% [**G2**] with $[\mathbf{II}]_0$ = 0.05 M under an N_2 atmosphere for 24 h. [b] Conversion of **II** was calculated by ^{1}H NMR analysis according to the norbornyl protons of **II**. [c] Incorporation of **I** was determined by ^{1}H NMR analysis according to the PEG signal of **I**.

the norbornyl skeleton (5.80 ppm) and the terminal $-CH_3$ of PE chains (0.84 ppm) could be identified. Repeated purification of the copolymer using acetone/H_2O ensured that there is no unreacted NB-PEG$_{1000}$-RGD (**Ia**) left. Thus, the chemical shift at 3.55 ppm due to PEG is indicative of PEGylated biomolecule incorporation into the final brush copolymer. However, separation of PE-based macromolecules is known to be extremely challenging and impractical on a large scale. Due to the very limited solubility of PE in common organic solvents at moderate temperatures, we are still investigating methods to separate unreacted **II** from **III**. It is heartening to note from our bioassays that the unreacted NB-SA-t PE$_{1400}$ (**IIa**) is non-cytotoxic. Furthermore, from the ^{1}H NMR, only a trace amount of the norbornyl protons (6.06 ppm) from NB-SA-t PE$_{1400}$ (**IIa**) was observed. ^{1}H NMR spectra for all other polymers and calculation of PE MM **I** conversion and PEGylated MM **II** incorporation can be found in the ESI.†

Gel permeation chromatography (GPC) analysis of polymers containing both very hydrophobic PE and highly polar PEG-peptide is challenging in terms of finding a suitable GPC eluent and temperature. Thus, it is understandable that establishment of a realistic MW distribution and measurement of the true MW of the polymers are expected to be difficult. The values of various absolute molecular weights shown in Table 3 were calculated on the assumption that the relation of the first-order equation holds between the measured logarithmic value of the absolute molecular weight and the holding time. A certain amount of granular insoluble components was observed in a sample solution of **IIIb** during the GPC operation. This is consistent with the relatively lower M_n of **IIIb** observed since the insoluble components were filtered away prior to the GPC operation. These insoluble components are likely to be the PE$_{5000}$-RGD copolymer of greater molecular size. Alongside these observations, it is also noteworthy that due to the limited solubility in solvents, there is no way to separate the unreacted NB-SA-t PE macromonomer from the final brush copolymer. However, since the NB-SA-t PE macromonomer is present in a very small amount, the effect on the GPC analyses is marginal for PE$_{1400}$ copolymers **IIIa** and **IIIc**. However, a slight degree of inaccuracy in the MW determination for PE$_{5000}$ copolymers **IIIb** and **IIId** is expected due to lower conversion in this ROMP reaction. Repeated washing of mixtures with acetone/H_2O is the method we currently use for further purification. Investigation on the feasible method for PE derivative separation is underway. GPC traces including peptide-based macromonomers **Ia–d** are shown in the ESI.†

Table 3 GPC data of NB-SA-t PE MMs II and copolymers III

Polymers	M_n [a] (KDa)	PDI	
1	NB-SA-t PE$_{1400}$ **IIa**	3.0	1.38
2	NB-SA-t PE$_{5000}$ **IIb**	4.2	2.41
3	PE$_{1400}$-RGD copolymer **IIIa**	5.7	12.78
4	PE$_{5000}$-RGD copolymer **IIIb**	6.4	3.49
5	PE$_{1400}$-(GPHyp)$_3$ copolymer **IIIc**	20.8	4.18
6	PE$_{5000}$-(GPHyp)$_3$ copolymer **IIId**	26.7	3.79

[a] Determined by HT-GPC in 1,2,4-trichlorobenzene at 160 °C.

3.2 Thermal stability

Upon synthesis and chemical characterization, thermal gravimetric analyses (TGA) of the copolymers were conducted to ascertain their thermal stability before we proceeded with filament extrusion and 3D printing of coupons for biovalidation (Fig. 4). From the representative TGA graph of **IIIa** [3], we can see improved thermal stability of the bioactive PE$_{1400}$-RGD copolymer **IIIa** [3], over that of pure RGD peptide [**1**] and the PEGylated peptide macromonomer (NB-PEG$_{1000}$-RGD) **Ia** [2]. It was observed that the pure RGD [1] starts degrading slightly above 100 °C, whereas **Ia** [2] shows a 2-phase mass loss between 200 and 350 °C, likely due to the loss of RGD followed by the degradation of PEG. On the other hand, **IIIa** [3] had only lost about 5% of its weight at around 400 °C, likely from RGD loss. The significant improvement in the thermal stability of **IIIa** over that of either pure RGD or **Ia** allows most material processing methods such as melt extrusion-based 3D printing to be used on **IIIa**. Apart from TGA analyses, inductively coupled plasma mass spectrometry (ICP-MS) analysis of the isolated brush copolymers was also carried out to check and ensure that the residual Ru content in the copolymers falls below 1 ppm (Table S3†) for their acceptable use in tissue-contact medical device fabrication.[30]

3.3 *In vitro* osteogenic activity

Osteogenic and BMP-2 binding properties are important in orthopaedic implant materials. BMP binding is important for both osteogenesis and chondrogenesis. Alkaline phosphatase (ALP) assays using C2C12 myoblast cells and BMP-2 were performed on the 3D-printed coupon **CIIIa** of PE$_{1400}$-RGD/UHMWPE (Fig. 5). The ALP activity of C2C12s cultured on the PE$_{1400}$-RGD/UHMWPE coupon **CIIIa** ("PE1kRGD") was over 20% higher than that of neat UHMWPE ("PE blank"), suggesting that the incorporation of bioactive PE$_{1400}$-RGD copolymer into UHMWPE improves the osteogenic differentiation of C2C12 murine myoblasts *in vitro*.

ALP activity of the C2C12 cells with BMP-2 was also analyzed on the 3D-printed PE$_{5000}$-peptide/UHMWPE coupons

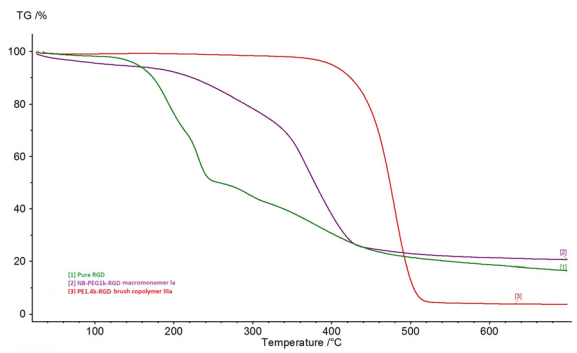

Fig. 4 TGA of pure RGD, **Ia** and **IIIa**.

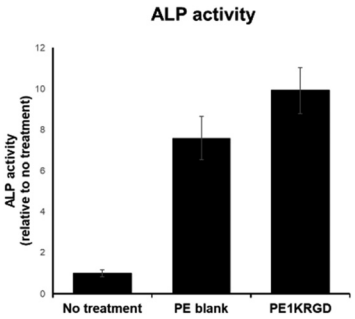

Fig. 5 ALP activity of C2C12 murine myoblast cells cultured on the 3D-printed PE_{1400}-RGD/UHMWPE coupon **CIIIa**.

CIIIb ("PE5k-RGD") and **CIIId** ("PE5k-GPHP") (Fig. 6). From the data, it is clear that all the 3D-printed coupons are able to support BMP-2-mediated ALP activity. However, little difference in ALP activity is observed between PE_{5000}-RGD/UHMWPE **CIIIb** ("PE5k-RGD") and PE_{5000}-mPEG/UHMWPE **CIVb** ("PE5k-mPEG") after the addition of BMP-2. The lower ALP activity improvement over neat UHMWPE ("PE-blank") in **CIIIb** may be due to lower RGD content in PE_{5000}-RGD/UHMWPE **CIIIb** since the blending with UHMWPE is by weight. Between PE_{5000}-RGD/UHMWPE **CIIIb** ("PE5k-RGD") and PE_{5000}-$(GPHyp)_3$/UHMWPE **CIIId** ("PE5k-GPHP"), it is clear that **CIIIb** ("PE5k-RGD") is able to enhance osteogenic activity more, indicating that the incorporation of RGD peptide into brush copolymer **III** is able to enhance BMP-2-mediated signals to a greater extent compared to that of the collagen fragment $(GPHyp)_3$. Based on the GPC characteristics of **IIId**, there is unseparated UHMWPE contained in the final **CIIId**, resulting in the poor ALP assay performance. The outcome here showed that PE_{5000}-$(GPHyp)_3$ **IIId** is less promising to be the additive for orthopaedic applications.

3.4 *In vivo* biocompatibility

In vivo biocompatibility evaluation of the 3D-printed PE_{5000}-peptide/UHMWPE coupons **CIIIb** and **CIIId** was performed using murine models. 3D-printed coupons **CIIIb** ("PE-RGD") and **CIIId** ("PE-GPHP") were inserted into the subcutaneous space under the skin *via* a small incision made on the upper dorsal back of the mouse. Histological analyses of the tissues at the implantation site after animal sacrifice at the end of week 4 showed increased inflammation of tissues due to the neat UHMWPE coupon ("PE-blank") (Fig. 7C and D) and **CIIId** coupon ("PE-GPHP") (Fig. 7G and H). Notably, a reduction in inflammation was observed for the **CIIIb** coupon ("PE-RGD") (Fig. 7E and F). This inflammation reduction of **CIIIb** ("PE-RGD") is important for its use in orthopaedic implants since the UHMWPE is a popular material for articulating surfaces of metal joint implants, but it is also known to cause significant inflammatory responses in the human body.[31,32] The ability of **IIIb** to reduce the inflammatory response *in vivo* and its ability to bind BMP-2 makes it a promising polymer additive for use in polyethylene-based orthopaedic implant materials.

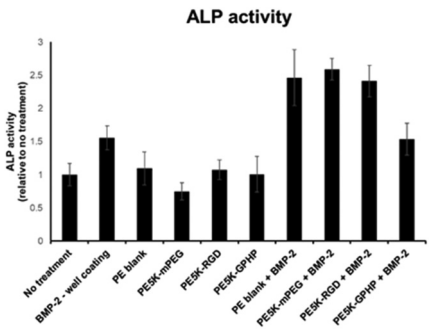

Fig. 6 ALP activity of C2C12 murine myoblast cells with BMP-2 cultured on the 3D-printed PE_{5000}-peptide/UHMWPE coupons **CIIIb** and **CIIId**.

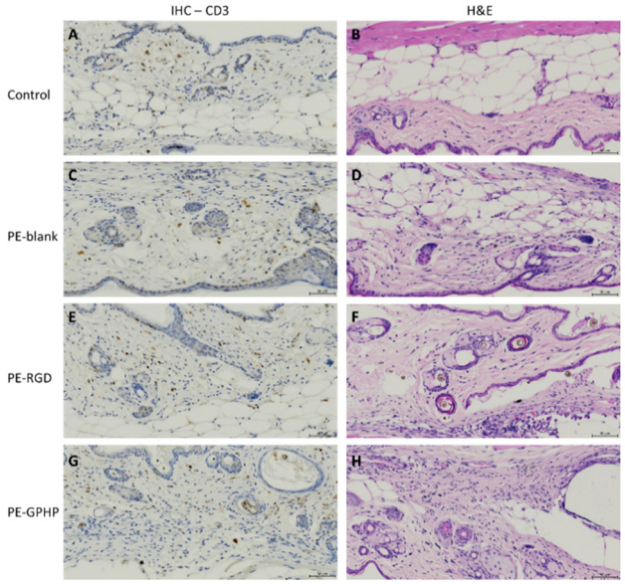

Fig. 7 Comparison of the bio-implanted murine skin tissues. (A, C, E and G) Immunohistochemical (IHC) staining for CD3 + cells, with cell nuclei (blue) and CD3 (brown) differentially labelled. (B, D, F and H) Haematoxylin and eosin (H&E) staining, with nuclear component (haematoxylin) and cytoplasmic components (eosin) differentially stained. Pathological assessment reports 2+ for (A and B) negative control, 3+ for (C and D) PE-blank, 2+ (E and F) PE-RGD and 3+ (G and H) PE-GPHP. All images shown are representative of at least 4 C57BL/6 mice per group. Scale bar = 50 μm.

4 Conclusions

In summary, we report a modular and efficient strategy for the synthesis of bioactive PE-peptide copolymers *via* ROMP. Synthesis and characterization of brush polymers containing PE side chains and PEGylated peptides have been presented. This method can potentially be extended to various peptides to provide access to versatile biofunctionalized brush copolymers. By incorporating integrin-binding peptides such as RGD

and collagen mimics such as $(GPHyp)_3$ into the PE-based brush copolymers, osteogenic activity and inflammatory response reduction could be introduced. The improvement of the thermal stability of the peptides in the brush copolymers allow these polymers to function as biomolecule carriers in high melting point UHMWPE. The reduction in inflammatory response and BMP-2 binding capability of our bioactive PE/UHMWPE formulation make the material an attractive candidate for use in PE-based orthopaedic devices such as articulating surfaces of joint implants. Optimization of formulations and further studies on the use of these bioactive PE materials using *in vivo* large animal models for tissue repair are ongoing.

Author contributions

All authors listed have made a substantial, direct, and intellectual contribution to the work, and approved it for publication.

Conflicts of interest

The authors declare no competing financial interest.

Acknowledgements

We acknowledge the generous support for this research from the Institute of Materials Research (IMRE) and Engineering and the Institute of Molecular and Cell Biology (IMCB), A*STAR, Singapore. This work was funded by Wound Care Innovation in the Tropics (grant H1701a00N9) and A*STAR GAP projects (ACCL190291, 200322). All succinic-acid terminated polyethylene and UHMWPE were obtained from Mitsui Chemicals Inc. (MCI) *via* materials transfer agreements between A*STAR and MCI. We thank Dr Wang Hongbo from the Mitsui Chemicals Singapore R&D Center, Dr Song Xiaolu from Jiangsu University, China, and Mr Heng Teck Huat from IMRE, for their contributions in the early phase of this work.

References

1 A. J. T. Teo, A. Mishra, I. Park, Y. J. Kim, W. T. Park and Y. J. Yoon, *ACS Biomater. Sci. Eng.*, 2016, **2**, 454–472.
2 A. Bharadwaz and A. C. Jayasuriya, *Mater. Sci. Eng., C*, 2020, **110**, 110698.
3 V. R. Sastri, in *3 - Materials Used in Medical Devices*, ed. V. R. Sastri, William Andrew Publishing, Oxford, 2014, pp. 19–31.
4 E. Zolotarevova, G. Entlicher, E. Pavlova, M. Slouf, D. Pokorny, F. Vesely, J. Gallo and A. Sosna, *Acta Biomater.*, 2010, **6**, 3595–3600.
5 A. Gigante, C. Bottegoni, V. Ragone and L. Banci, *J. Funct. Biomater.*, 2015, **6**, 889–900.
6 U. Hersel, C. Dahmen and H. Kessler, *Biomaterials*, 2003, **24**, 4385–4415.
7 R. Langer, Biomaterials in Drug Delevery and Tissue Engeneering: One Laboratory's Experience, *Acc. Chem. Res.*, 2000, **33**, 94–101.
8 I. M. Weiss, C. Muth, R. Drumm and H. O. K. Kirchner, *BMC Biophys.*, 2018, **11**, 2.
9 S. L. Perry, *Curr. Opin. Colloid Interface Sci.*, 2019, **39**, 86–97.
10 P. M. Stephen and A. H. Jeffrey, An RGD spacing of 440 nm is sufficient for integrin alpha V beta 3- mediated fibroblast spreading and 140 nm for focal contact and stress fiber formation, *J. Cell Biol.*, 1991, **114**(5), 1089–1100.
11 P. R. Patel, R. C. Kiser, Y. Y. Lu, E. Fong, W. C. Ho, D. A. Tirrell and R. H. Grubbs, *Biomacromolecules*, 2012, **13**, 2546–2553.
12 S. Y. Yoo, M. Kobayashi, P. P. Lee and S. W. Lee, *Biomacromolecules*, 2011, **12**, 987–996.
13 H. Ceylan, S. Kocabey, H. Unal Gulsuner, O. S. Balcik, M. O. Guler and A. B. Tekinay, *Biomacromolecules*, 2014, **15**, 2407–2418.
14 K. M. Hennessy, B. E. Pollot, W. C. Clem, M. C. Phipps, A. A. Sawyer, B. K. Culpepper and S. L. Bellis, *Biomaterials*, 2009, **30**, 1898–1909.
15 G. Bohn, B. Liden, G. Schultz, Q. Yang and D. J. Gibson, *Adv. Text. Wound Care*, 2016, **5**, 1–10.
16 A. Borodovsky, H. Ovaa, N. Kolli, T. Gan-Erdene, K. D. Wilkinson, H. L. Ploegh and B. M. Kessler, Chemistry-Based Functional Proteomics Reveals Novel Members of the Deubiquitinating Enzyme Family, *Chem. Biol.*, 2002, **9**, 1149–1159.
17 E. M. Kolonko, J. K. Pontrello, S. L. Mangold and L. L. Kiessling, General Synthetic Route to Cell-Permeable Block Copolymers via ROMP, *J. Am. Chem. Soc.*, 2009, **131**(21), 7327–7333.
18 K. Lienkamp, A. E. Madkour, A. Musante, C. F. Nelson, K. Nusslein and G. N. Tew, Antimicrobial polymers prepared by ROMP with unprecedented selectivity: a molecular construction kit approach, *J. Am. Chem. Soc.*, 2008, **130**(30), 9836–9843.
19 Y. C. Teo, E. J. Park, J. Guo, A. Asyraf, A. Smith, D. Goh, J. P. S. Yeong, S. Cool and P. Teo, *ACS Appl. Bio Mater.*, 2022, **5**(10), 4770–4778.
20 V. Héroguez, A. Chemtob and D. Quemener, in *ROMP in Dispersed Media*, 2015, pp. 25–44.
21 C. Slugovc, in *Synthesis of Homopolymers and Copolymers*, 2015, pp. 1–23.
22 J. B. Matson and R. H. Grubbs, Synthesis of Fluorine-18 Functionalized Nanoparticles for Use as in Vivo Molecular Imaging Agents, *J. Am. Chem. Soc.*, 2008, **130**, 6731–6733.
23 H. D. Maynard, S. Y. Okada and R. H. Grubbs, Synthesis of Norbornenyl Polymers with Bioactive Oligopeptides by Ring Opening Metathesis Polymerization, *Macromolecules*, 2000, **33**(17), 6239–6248.
24 A. V. Sesha Sainath, M. Isokawa, M. Suzuki, S. Ishii, S. Matsuura, N. Nagai and T. Fujita, *Macromolecules*, 2009, **42**, 4356–4358.

25 M. S. Sanford, J. A. Love and R. H. Grubbs, Mechanism And Activity Of Ruthenium Olefin Metathesis Catalysts, *J. Am. Chem. Soc.*, 2001, **123**, 6543–6554.
26 Y. V. Dontsov, S. V. Panin, D. G. Buslovich and F. Berto, *Materials*, 2020, 13.
27 C. R. Rocha, A. R. Torrado Perez, D. A. Roberson, C. M. Shemelya, E. MacDonald and R. B. Wicker, *J. Mater. Res.*, 2014, **29**, 1859–1866.
28 R. A. A. Smith, S. Murali, B. Rai, X. Lu, Z. X. H. Lim, J. J. L. Lee, V. Nurcombe and S. M. Cool, *Biomaterials*, 2018, **184**, 41–55.
29 H. Zhang and N. Hadjichristidis, *Macromolecules*, 2016, **49**, 1590–1596.
30 ICH guideline Q3D (R1) on elemental impurities 2019, March 22.
31 I. Fernandez-Bueno, S. Di Lauro, I. Alvarez, J. C. Lopez, M. T. Garcia-Gutierrez, I. Fernandez, E. Larra and J. C. Pastor, *J. Ophthalmol.*, 2015, 904096.
32 E. Gibon, L. A. Cordova, L. Lu, T. H. Lin, Z. Yao, M. Hamadouche and S. B. Goodman, *J. Biomed. Mater. Res., Part B*, 2017, **105**, 1685–1691.